

Zero Voltage Switching Switched-Tank Modular Converter for Data Center Application

Mengxuan Wei^a, Yanchao Li^b, Ze Ni^c, Chengkun Liu^a, Dong Cao^a

Electrical and Computer Engineering Department

a.University of Dayton, Dayton , Ohio, United States

b.AZ power. INC, Culver City, California, United States

c. North Daota State University, Fargo, North Dakota, United States

dcao02@udayton.edu

Abstract— Recently, Switched-tank converter (STC) using zero current switching (ZCS) for 48 V-12 V data center application has reached 98.55% efficiency. However, the C_{oss} loss is not recycled and it increases with frequency and voltage. This paper describes a switched-tank modular (STM) converter with zero voltage switching (ZVS) for all devices over full load range. It can eliminate C_{oss} loss and further improve efficiency. Different from traditional STC, the STM is more modularized and much easier to be integrated into high voltage application. Besides, the STM converter has smaller clamping capacitance compared with large clamping capacitor in traditional STC. As a result, higher efficiency and power density can be achieved. In this paper, the ZVS operation for STM converter is discussed. Also, the efficiency and power loss comparison using GaN and Si devices is analyzed. The simulation and experiment results based on a Si prototype are presented.

Keywords—switched-tank modular converter, zero-voltage switching, dc-dc converter

I. INTRODUCTION

With the rapid development of the internet service such as cloud computing and big data, the power consumption for data center have dramatically increased. Electric consume for data center is more than 1.8% in 2014 and will raise to 73 billion kWh by 2020[1][2]. Therefore, handling the increasing server computing capability and minimizing the energy usage of data center at the same time is a new trend. As a result, in order to shrink the electricity bill, efficiency improvement has been well studied these days. Due to high-efficiency feature, dc distribution system is adopted to replace the traditional ac system for data center.[3] Thanks to the fast development of wide-bandgap device, it offers a new choice for the power electronics application.[4] By utilizing the wide-bandgap device, the converter can be operating at a faster speed with smaller volume. For the better system efficiency, the 48 V intermediate bus architecture (IBA) has been widely adopted in modern data centers[5].

Recently, many works have been done to improve the 48 V-12 V IBA bus converter efficiency. Switched-tank converter (STC) was first introduced in [6][7]. It is derived from the switched-capacitor concept which allows the increase of efficiency and power density with minimize the size of the passive component. [8]-[12]. The STC with zero current switching (ZCS) operation reaches 98.55% efficiency and the C_{oss} loss is the dominator at light load. It is more suitable for the low voltage high current application and not able to achieve full zero voltage switching (ZVS). In order to further improve the efficiency to 98.71%, the on-time control is discussed in [13]. Expect STC, in [14], cascaded resonant switched-capacitor converter (CRSCC) is proposed and can

reach 98.9% high efficiency under ZCS operation. To further decrease power loss of CRSCC, [15] utilize the ZVS control for CRSCC and it achieves ZVS for all devices and increase the efficiency to 99%, but the switching frequency is only 100 kHz, which doesn't fully utilize the high-speed switching capability of the devices. The comparison of STC and CRSCC is detail analyzed in [16]. The Transformerless stacked active bridge (TSAB) converter [17] is derived by inserting a small ac inductor into Dickson SC converter [18] It achieves partial ZVS, but the peak efficiency is 98.6% at only 30 W. The transformer-less quadruple active half-bridge (QAHB) is proposed in [19]. It can realize ZVS on all switching devices, but the peak efficiency is 98.4%. ZVS Switched Capacitor Converter (ZSC) that derived from the STC is proposed in [20] and it reaches the peak efficiency 99%. In this paper, a switched-tank modular (STM) converter is proposed and it can achieve ZVS on all services. By applying ZVS control, the C_{oss} loss, which is a big concern with high frequency and voltage condition, is recycled. The STM converter have several benefits such as only uses devices with voltage stress equal to the output voltage which is more modularized and much easier to be integrated into high voltage application. Also, the STM converter has smaller clamping capacitance compared with large clamping capacitor in traditional STC.

This paper contains three parts. Section II discuss the ZVS operation principles of the STM converter while the loss modeling and efficiency analysis based on Si and GaN device is presented in Section III. The Section IV shows the simulation and the experiment results. Finally, Section V concludes the paper.

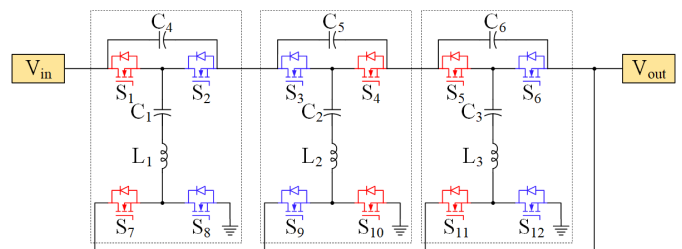


Fig. 1. Switched-tank Modular Converter Topology

II. OPERATING PRINCIPLES OF THE STM CONVERTER

The schematic drawing of the four times conversion ratio (4x) switched-tanked modular converter is shown in Fig.1. In this topology, half bridges are used as the basic blocks. Two half bridge blocks, a clamping capacitor and a LC tank makes up a module. A converter with N times conversion ratio will need $N+1$ module. When the device switching frequency

equals to the frequency of the LC tank, $f_s = f_r = \frac{1}{2\pi\sqrt{LC}}$, the converter is working under the ZCS operation. Similar to switched-tank converter, the ZCS operation mode for the switched-tanked modular converter have two working states. The two complementary control signals turn on the red devices and blue device in sequence for ZCS operation.

Comparing to ZCS, ZVS can improve the light-load efficiency further by reducing the switching C_{oss} recycling the energy from MOSFET output capacitance. The realization of ZVS for switched-tanked modular converter requires that the switching frequency is higher than the resonance frequency, $f_s > f_r = \frac{1}{2\pi\sqrt{LC}}$. The corresponding control signals for ZVS operation are presented in Fig.2. S_r and S_b are two complementary control signals for the upper side red and blue devices respectively. Similarly, S_{rr} and S_{bb} are control signal for bottom side red and blue devices. There is a phase shift angle between S_r and S_{rr} , S_b and S_{bb} . To achieve ZVS turn on for the device, the requirement is that the body diode conducts before the device turns on. To meet this requirement, during the turn-on period, the device current should flow from source to drain.

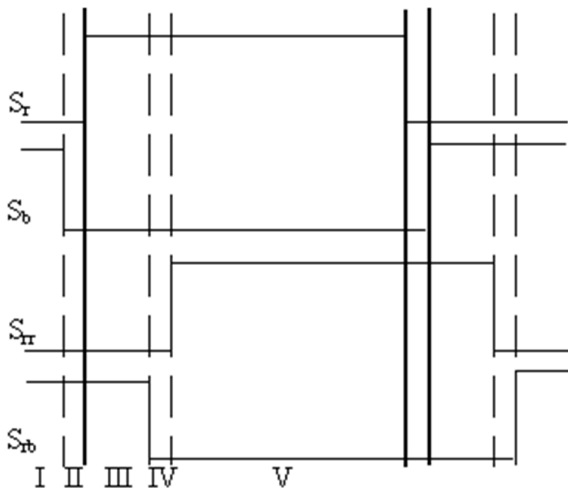


Fig. 2. Control Signal for ZVS Operation

There are two steady-state mode, i.e. Mode I and Mode V as shown in Fig 3(a)(e). In the mode I, all the blue devices are conducting, while in mode V all the red devices stay on. Between the two modes are three ZVS turn on transient modes. The ZVS turn-on process consists of Mode II~IV. Fig.3 (b)(c)(d) shows the three ZVS equivalent circuits. The grey dashed and color solid line devices are off and on, respectively in the corresponding modes. While, colored dashed devices prepare for ZVS turn on. As shown in Fig.3 (b), at the start of the mode II, the S_2 , S_3 , S_6 turns off and the S_8 , S_9 , S_{12} continue conducting. During this mode, the output capacitor of the S_1 , S_4 , S_5 are discharging to prepare for the ZVS turn on. In (c), at the beginning of the mode III, the S_1 , S_4 , S_5 ZVS turned on and the S_8 , S_9 , S_{12} continue conducting. In this mode, the inductor current changed directions. In mode IV, S_8 , S_9 , S_{12} turns off at the start, S_7 , S_{10} , S_{11} output capacitor is discharging. To achieve this ZVS operation, make sure that the inductors have enough energy to charge and discharge the device output capacitances.

Table I shows the comparation of different topologies which are developed from switched-capacitor concept. According to the control strategy, CRSCC and switched-tank

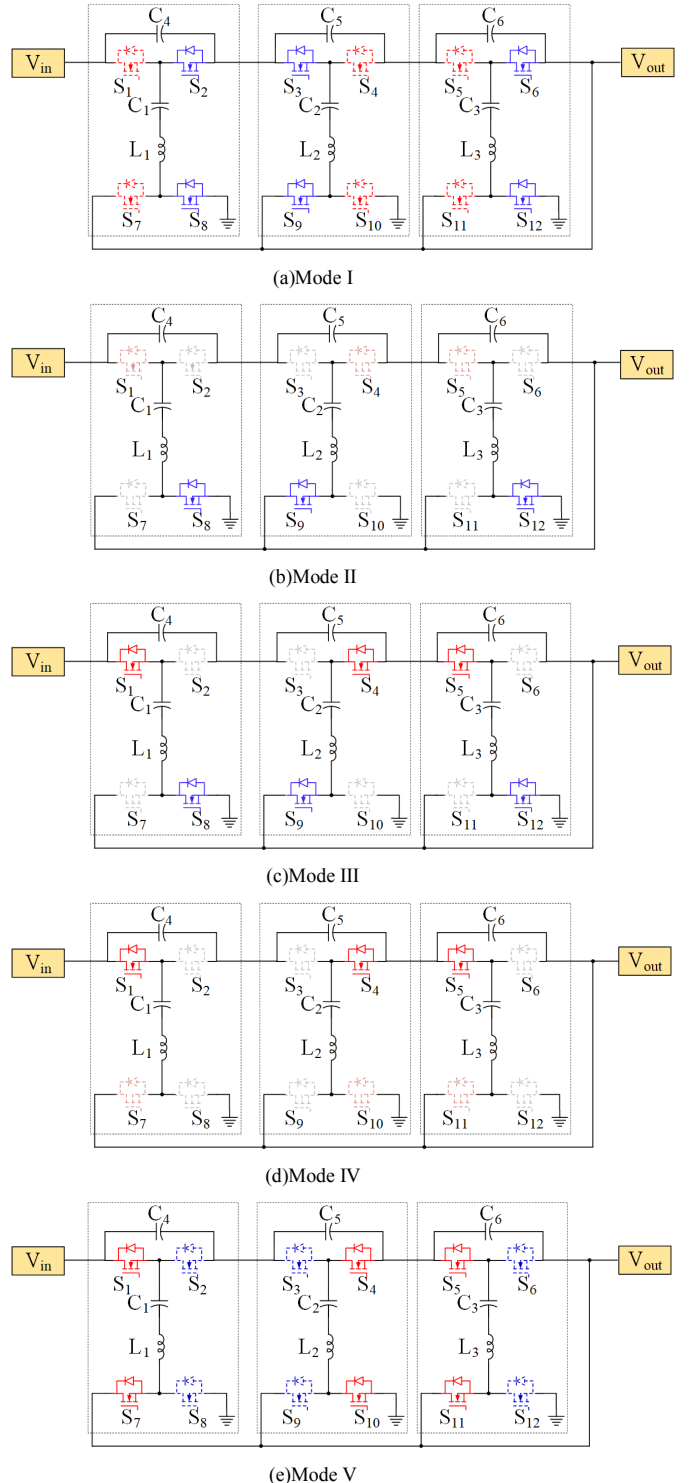


Fig. 3. ZVS Operation Equivalent Circuit

modular converter can both operate at ZCS and ZVS operation however STC can only operate at ZCS and TSAB can operate at ZVS. Assume the low current stress device is the device that RMS current is V_{out}/R_{load} . When considering about the device current stress, CRSCC have four high currents dress device used and the TSAB utilize two high current devices in the topology, however, for the STC and switched-tank modular converter, all the devices are low current dress device.

TABLE I. COMPARISON OF SEVERAL TOPOLOGIES WITH 4-TO-1 CONVERSION RATIO

Converter	Control Strategy	Device Current Stress	Device Voltage Stress	Scalability
CRSCC	ZCS, ZVS	4 High current stress devices	4 High voltage stress devices	Average
		4 Low current stress devices	4 Low voltage stress devices	
STC	ZCS	10 Low current stress devices	2High voltage stress devices	Average
			8 Low voltage stress devices	
TSAB	ZVS	2 High current stress devices	2High voltage stress devices	Average
		6 Low current stress devices	6 Low voltage stress devices	
STM	ZCS, ZVS	12 Low current stress devices	12 Low voltage stress devices	Good

Similarly, by defining the device voltage stress equals V_{out} as the low voltage stress device. For the device voltage stress CRSCC have four high voltage dress devices, TSAB and STC both have two high voltage stress DEVICES, all the device in switched-tank modular convert are low voltage stress device. Because of these features, the switched-tank modular converter has the best scalability

III. EFFIENCY ANALYSIS AND DEVICE COMPARASION

The power loss on the semiconductor device contains three parts: the gate driver loss (P_{gate}), the output capacitor loss(P_{coss}) and the conduction loss(P_{cond}). When the switched-tank modular converter is working at ZVS mode, the P_{coss} is recycled. Thus, the total power loss on the semiconductor device(P_{semi}) is the sum of gate driver loss and conduction loss, as shown in (1)

$$P_{semi} = P_{gate} + P_{cond} \quad (1)$$

- Gate drive loss: The gate drive loss can be calculated using (2), where V_{gs} is the gate drive voltage, Q_g is total gate charge, and f_s is devices switching frequency.
- Conduction loss: The conduction loss can be calculated using (3), The drain-to-source on state resistance of one device is $R_{ds(on)}$. The root mean square (RMS) value of current flow through it.

$$P_{gate} = V_{gs} Q_g f_s \quad (2)$$

$$P_{cond} = i_{rms}^2 \times R_{ds(on)} \quad (3)$$

When working in the extreme case, the input voltage will be 60V, all the devices have the maximum voltage, for the 4 to 1 conversion ratio topology, it is 15V. As a result, to build the converter, several types of switching devices which have 25V or 30V voltage rating are compared. For GaN devices, the EPC have 30V voltage rating MOSFET available. For Si device, Infineon optimos5 provide both 25V and 30V MOSFET.

Since higher gate driver voltage can result in a lower MOSFET on-state resistance which can reduced conduction loss and cause higher gate driver loss at the same time. For the GaN device, the 5 V gate driver voltage is the only choice, however, Infineon optimos5 Si device have wild range of gate driver voltage. To make sure that the comparison is fair enough, assume the gate driver voltage for all devices are 5V. Besides, to purely compared switching device loss, the inductor loss, capacitor loss and the PCB loss are assumed the

same when the converter is operating in the same condition. This analysis includes four Si MOSFETs and one eGaNFET that have either low $R_{ds(on)}$ or Q_g among 25V and 30 V devices. Their key parameters used in the analysis can be found in Table II

TABLE II. PARAMETERS OF SWITCHING DEVICES USED IN ANALYSIS

Part#	Rating	V_{gs} (V)	Q_g (nC)	$R_{ds(on)}$ (mΩ)
BSZ031NE2LS5	25V 40A	5	6.5	3.1
BSZ013NE2LS5I	25V 40A	5	16	1.25
BSZ017NE2LS5I	25V40A	5	11	1.78
BSZ014NE2LS5IF	25V 40A	5	11.3	1.5
EPC2023	30V 90A	5	19	1.15

Fig.4 shows the efficiency curve over all load range when switched-tank modular converter utilizing these five types of MOSFET. As shown in Fig.4 the BSZ031NE2LS5 has the highest peak efficiency at the light load. In the light load circumstances, the gate drive loss will be the dominator for the semiconductor power loss. Due to the small Q_g , the gate drive loss for BSZ031NE2LS5 is the smallest. This cause the highest peak efficiency at light load. However, for the full load efficacy circumstances, the conduction loss becomes the dominator for the semiconductor device power loss. because the increase of the current flow though the device. Since the BSZ031NE2LS5 has a relatively large $R_{ds(on)}$, the efficiency at full load is lowest. For the EPC2023 and BSZ013NE2LS5I, the performance is nearly the same over all load range but BSZ013NE2LS5I has a higher peak efficiency

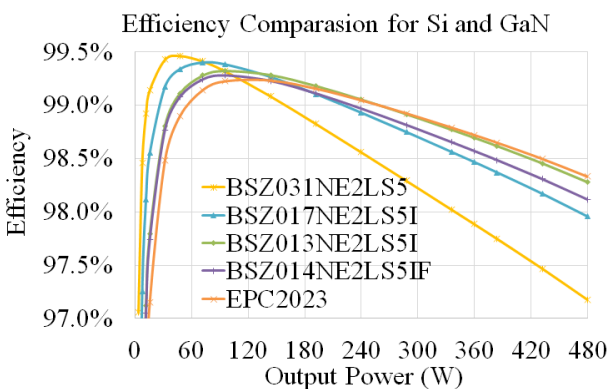


Fig. 4. Efficiency Comparasion on Different Device (Si and GaN)

Detailed breakdown comparison for the two device power loss is shown in (b). Since the gate drive loss only related to V_{gs} , f_s and Q_g , these values are fixed for the fixed condition. Therefore, GaN devices have larger Q_g than Si devices under full load range. For the conduction loss, the GaN device have a slightly better performance for the conduction loss due to the smaller $R_{ds(on)}$. Thus, during the light load, the conduction loss is not the dominator of the power loss and Si device have less power loss which result in a higher peak efficiency. Under the full load conduction, since the $R_{ds(on)}$ difference between Si devices and GaN devices is quite small, even though the conduction loss is the dominator, the efficiency is nearly the same. Base on all these consideration, the BSZ013NE2LS5I will be the most suitable device to use.

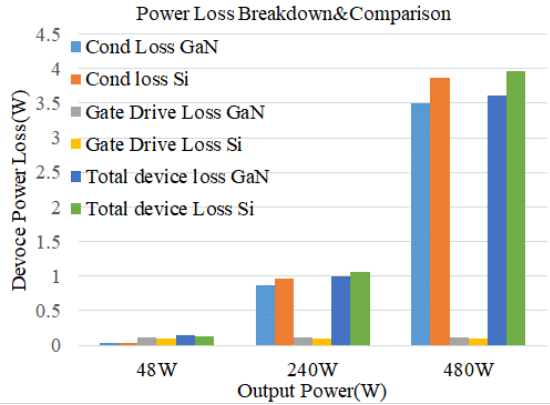


Fig. 5. Power Loss Breakdown Comparison between Si and GaN

IV. SIMULATION AND EXPERIMENTAL RESULT

Simulation studies of the 4-to-1 switched-tank modular converters with PLECS is conducted. The simulation parameter is shown in table III.

TABLE III. PARAMETER USED IN SIMULATION

Items	Symbols	Values
Switching Frequency	f_s	350kHz
Input Voltage	V_{in}	48V
Output Voltage	V_{out}	12V
Resonant Inductance	L_r	36nH
Resonant Capacitance	C_r	35μF
Device On-state Resistance	$R_{ds(on)}$	1.25mΩ
Device Output Capacitance	C_{oss}	1.8nF

In Fig.6, the first and second plot shows the voltage and current waveform for the top and bottom device respectively. As shown in the plot, the voltage across the device reach zero before the device starts conducting. Thus, the ZVS operation is achieved both for the top and bottom devices. The last plot shows the inductor current for L_1 and L_2 and it also reflects the realization of ZVS operation.

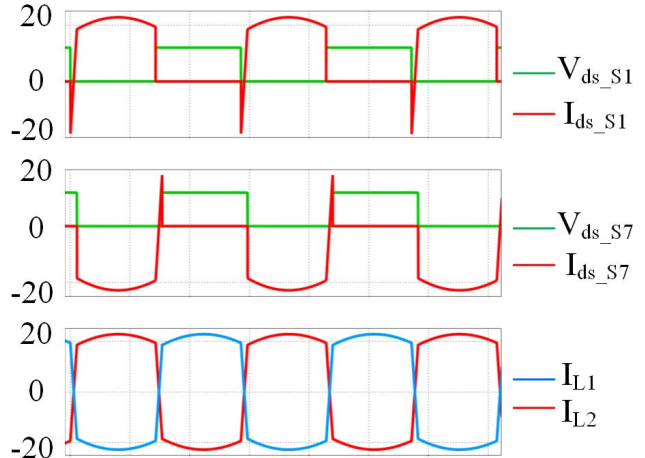


Fig. 6. Simulation Result at Full Load

Due to the relocation of the lab, the test bench is unable to set up for testing the proposed converter and verify the analysis result. However, a similar concept converter, Switched-capacitor Resonant Converter (SCRC), prototype is built, and the testing result can prove the analysis in some way. The topology is shown below in Fig.7. The change of this topology is using two high voltage stress devices to replace four low voltage stress devices. It has similar working performance when it is also operating at ZVS.

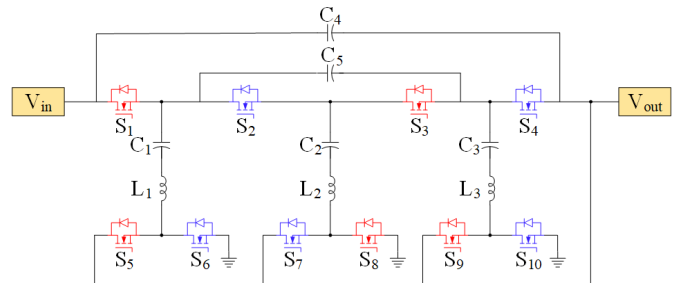


Fig. 7. SCRC Topology

Since SCRC use less device than the switched-tank modular converter, the efficiency for the SCRC will be higher than switched-tank modular converter. By applying the same efficiency analysis model and set the parameters such as the switching frequency, the resonant inductance and resonant capacitance the same value, the relationship of the two converter is shown in Fig.8. Based on the analysis result, the peak efficiency for the SCRC is 99.49% and for the switched-tank modular converter is 99.35%

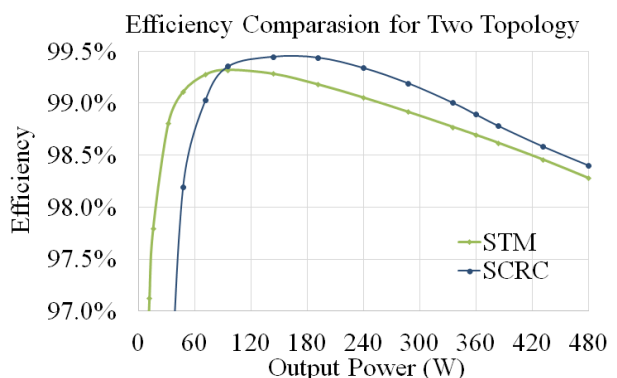


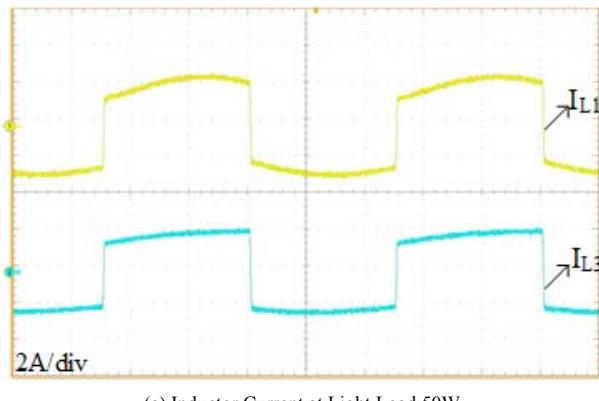
Fig. 8. Analysis Efficiency of Two Converters

The prototype is shown in Fig.9. The input voltage for the test is 48V and the output is 12V. The converter working with the switching frequency at 200kHz. Fig.10 show the experiment result for the inductor current under the light load 50W(a) and heavy load 450W(b). The inductor waveform indicates that the converter achieves the ZVS.

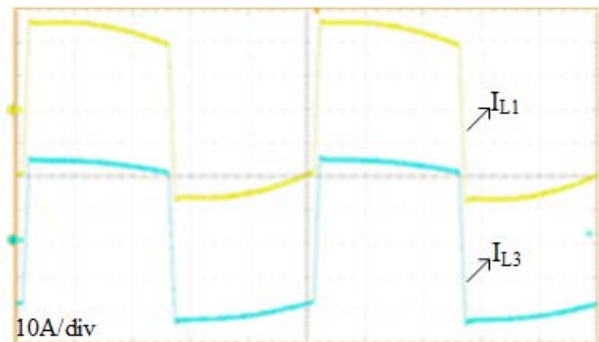
The Fig.11 show the measured efficiency for the SCRC and compare it with other same function converters such as CRSSCC, TSAB and ZSC. By inheriting the relationship from the analysis result, the efficiency of switched-tank modular converter can also be predicted, and it is also shown in the graph.



Fig. 9. Prototype of 4-to-1 SCRC



(a) Inductor Current at Light Load 50W



(b) Inductor Current at Heavy Load 450W

Fig. 10. Experiment result for 4-to-1 SCRC

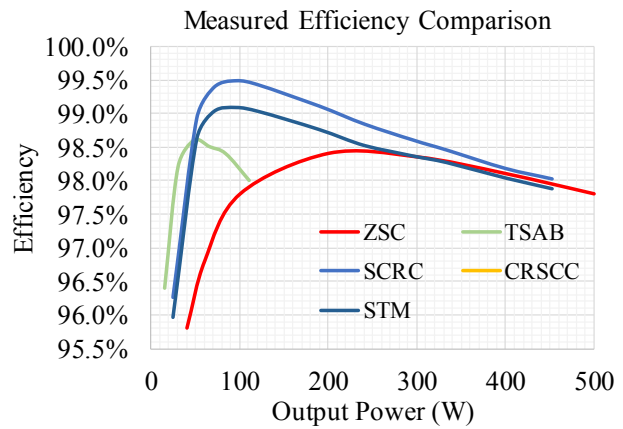
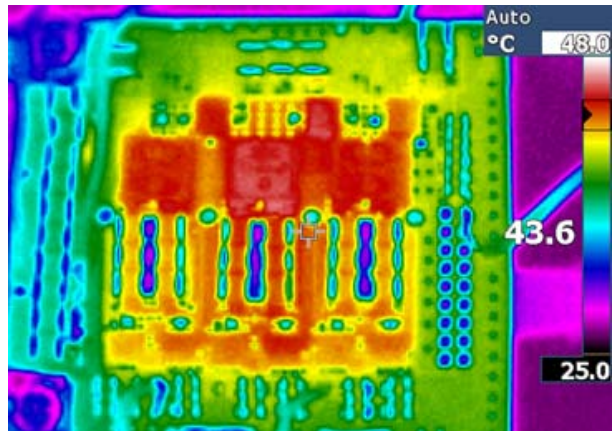


Fig. 11. Measured Efficiency Comparison Between Different Topology

The thermal performance of the prototype at 450W is shown in Fig.13. The environment temperature is 25 °C and a fan is used for cooling. The highest temperature showed is 48°C and it occurs near the high voltage stress device. The typical temperature of the board is 43.6°C and is close to the highest temperature. This reflects that the high-efficiency design contribute the excellent thermal performance.



V. CONCLUSION

This paper presents the switched-tank modular converter derived from the traditional switched-tank converter. This converter not only inherit all the feature of the STC but also the ZVS operation can be achieved. By applying the ZVS control, the light load efficiency is greatly improved. Besides the increase of the peak efficiency, the switched-tank modular converter also has good scalability which allows the topology apply for the high voltage application. The experiment and analysis result shows the excellent performance of the switched-tank modular converter. It indicates that this topology can be adopted as a good option for the data center application where the high efficiency high density power delivery is a key factor.

REFERENCES

- [1] M. Dayarathna, Y. Wen, and R. Fan, "Data center energy consumption modeling: A survey," IEEE Commun. Surveys Tuts., vol. 18, no. 1, pp. 732–794, Firstquarter 2016
- [2] A. Shehabi et al., "United states data center energy usage report," Lawrence Berkeley National Laboratory, Berkeley, CA, Tech.Rep.LBNL-1005775, Aug, 2016. [Online]. Available: https://datacenters.lbl.gov/sites/default/files/DCDWebscale_Shehabi_072016.pdf

- [3] G. Eason Department of Energy, "Data Center Energy Efficiency," 2016.[Online].Available:https://energy.gov/sites/prod/files/2016/07/f3/3/dc_improvement.pdf
- [4] A. Elasser and T. P. Chow, "Silicon carbide benefits and advantages for power electronics circuits and systems," in Proceedings of the IEEE, vol. 90, no. 6, pp. 969-986, June 2002
- [5] S. Mills, "Overview of Open Rack Standard V2.0," in Proc. OCP Eng. Workshop, 2016, pp. 1-28. [Online]. Available:<http://files.opencompute.org/oc/public.php?service=files&t=cf80ec91104554a01b3227983f3a89c>. Accessed on: Feb. 8, 2017
- [6] Y. Li, X. Lyu, D. Cao, S. Jiang and C. Nan, "A 98.55% Efficiency Switched-Tank Converter for Data Center Application," in IEEE Transactions on Industry Applications, vol. 54, no. 6, pp. 6205-6222, Nov.-Dec. 2018.
- [7] S. Jiang, S. Saggini, C. Nan, X. Li, C. Chung, and M. Yazdani, "Switched tank converters," IEEE Transactions on Power Electronics, 2018
- [8] M. S. Makowski and D. Maksimovic, "Performance limits of switched-capacitor DC-DC converters," in Proc. IEEE PESC, 1995, vol. 2, pp. 1215-1221.
- [9] K. D. T. Ngo and R. Webster, "Steady-state analysis and design of a switched-capacitor DC-DC converter," IEEE Trans. Aerosp. Electron. Syst., vol. 30, no. 1, pp. 92-101, Jan. 1994
- [10] M. D. Seeman and S. R. Sanders, "Analysis and optimization of switched-capacitor DC-DC converters," IEEE Trans. Power Electron., vol. 23, no. 2, pp. 841-851, Mar. 2008
- [11] D. Cao and F. Z. Peng, "Zero-current-switching multilevel modular switched-capacitor DC/DC converter," IEEE Trans. Ind. Appl., vol. 46, no. 6, pp. 2536-2544, Nov. 2010
- [12] Y. Lei, W. C. Liu, and R. C. N. Pilawa-Podgurski, "An analytical method to evaluate and design hybrid switched-capacitor and multilevel converters," IEEE Transactions on Power Electronics, vol. PP, no. 99, pp. 1-1, 2017
- [13] Y. Li, X. Lyu, Z. Ni, D. Cao, C. Nan and S. Jiang, "Adaptive On-Time Control for High Efficiency Switched-Tank Converter," 2018 1st Workshop on Wide Bandgap Power Devices and Applications in Asia (WiPDA Asia), Xi'an, China, 2018, pp. 169-175.
- [14] Z. Ye, Y. Lei and R. C. N. Pilawa-Podgurski, "A resonant switched capacitor based 4-to-1 bus converter achieving 2180 W/in³ power density and 98.9% peak efficiency," 2018 IEEE Applied Power Electronics Conference and Exposition (APEC), San Antonio, TX, 2018, pp. 121-126
- [15] Z. Ye, Y. Lei and R. C. N. Pilawa-Podgurski, "A 48-to-12 V Cascaded Resonant Switched-Capacitor Converter for Data Centers with 99% Peak Efficiency and 2500 W/in³ Power Density," 2019 IEEE Applied Power Electronics Conference and Exposition (APEC), Anaheim, CA, USA, 2019, pp. 13-18
- [16] X. Lyu, Y. Li, D. Cao, S. Jiang and C. Nan, "Comparison of GaN based switched-tank converter and cascaded voltage divider," 2017 IEEE 5th Workshop on Wide Bandgap Power Devices and Applications (WiPDA), Albuquerque, NM, 2017, pp. 158-164.
- [17] J. Zhu and D. Maksimović, "A Family of Transformerless Stacked Active Bridge Converters," 2019 IEEE Applied Power Electronics Conference and Exposition (APEC), Anaheim, CA, USA, 2019, pp. 19-24.
- [18] J. F. Dickson, "On-chip high-voltage generation in mnos integratedcircuits using an improved voltage multiplier technique," IEEE Journal of solid-state circuits, vol. 11, no. 3, pp. 374-378, 1976
- [19] S. Khatua, D. Kastha and S. Kapat, "A Transformer-Less Quadruple Active Half-Bridge Converter for the Two-Stage 48V VRM Application," 2019 IEEE Applied Power Electronics Conference and Exposition (APEC), Anaheim, CA, USA, 2019, pp. 488-495.
- [20] M. Hunter, M.Chen, C.Rainer, Y.Zhou and R. Renganathan, "ZVS Switched Capacitor (ZSC) Converter for Future Data Center Applications"2019 IEEE Applied Power Electronics Conference and Exposition (APEC), Anaheim, CA, USA, 2019